Interpretation of Electron Scattering Experiments*†

L. I. SCHIFF
Stanford University, Stanford, California

(Received June 26, 1953)

Experiments on the elastic scattering of fast electrons by several elements, reported by Hofstadter, Fechter, and McIntyre in the preceding paper, are interpreted with the help of the first Born approximation. This interpretation of the experiments implies nuclear charge distributions that are peaked at the center and taper off smoothly. The root-mean-square radii of the charge distributions, and the nuclear Coulomb energies, are, however, in approximate agreement with those computed from the usual uniform charge distribution. The effects of radiation loss and nuclear excitation are discussed qualitatively, and the effect of a nuclear electric quadrupole moment is considered more quantitatively. It is concluded that these effects probably cannot account for the discrepancy between the observed scattering cross section which decreases monotonically with increasing angle and the diffraction minima and maxima expected on the basis of the Born approximation from a uniform charge distribution with a sharp or moderately rounded edge. Exact calculations of the elastic scattering from various charge distributions are now under way.

1. INTRODUCTION

THE preceding paper by Hofstadter, Fechter, and McIntyre[1] reports experimental results on the elastic scattering of fast electrons by several elements. The energy resolution of the incident and scattered electrons is such that the measured differential cross sections include both elastic events and inelastic events in which the energy loss to radiation or nuclear excitation is less than about 1 Mev, after allowance is made for the recoil energy of the struck nucleus. The observed monotonic decrease of the scattering cross section with increasing angle is in striking contrast with the diffraction minima and maxima calculated by means of the Born approximation[2] when the nuclear charge is assumed to be roughly uniformly distributed over a sphere of approximate radius $1.4\times10^{-13}A^{\frac{1}{3}}$ cm. While the first Born approximation is not reliable for heavy elements such as tantalum, gold, and lead, it should give a qualitative indication of the general character of the scattering for various assumed forms of the nuclear charge distribution. This view is confirmed by exact scattering calculations now in progress,[3a] which show that the principal effect of the improvements on the Born approximation in the case of a uniformly charged nucleus is the filling in of the zeros in the cross section to convert the minima and maxima into wiggles. This effect was noted earlier by M. Goldhaber and A. W. Sunyar [Phys. Rev. **83**, 906 (1951)].

All of the calculations in this paper are based on the first Born approximation. This enables us to make a rapid survey of the qualitative effect of the form of the nuclear charge distribution on the elastic scattering, and also to estimate the relative importance of inelastic processes and of the nuclear distortion implied by the existence of electric quadrupole moments. The results obtained cannot be taken literally for the heavy elements, but are expected to be more reliable for lighter elements and quite good for beryllium and deuterium.

2. USE OF THE FIRST BORN APPROXIMATION

For an electron of energy E that is scattered by a nucleus that is represented by wave functions Ψ_i, the differential scattering cross section per unit solid angle is[2]

$$\sigma(\theta)=[(4e^4E^2\cos^2\tfrac{1}{2}\theta)/(\hbar cq)^4]\times\left|\int\Psi_f^*\sum_{k=1}^{Z}e^{i\mathbf{q}\cdot\mathbf{R}_k}\Psi_i d\tau\right|^2, \quad (1)$$

where $\hbar\mathbf{q}$ is the momentum transfer from the electron to the nucleus that makes a transition from state i to state f, and $\mathbf{R}_k$ is the coordinate of a proton in the nucleus; it is assumed that E is large in comparison with the rest energy of the electron, and that the scattering angle θ is not close to π. For elastic scattering, $q=(2E/\hbar c)\sin\frac{1}{2}\theta$, and Eq. (1) can be written in one of the forms

$$(e^4\cos^2\tfrac{1}{2}\theta/4E^2\sin^4\tfrac{1}{2}\theta)\left|\int\sum_{k=1}^{Z}|\Psi_i|^2e^{i\mathbf{q}\cdot\mathbf{R}_k}d\tau\right|^2 = (Z^2e^4\cos^2\tfrac{1}{2}\theta/4E^2\sin^4\tfrac{1}{2}\theta)\left|\int\rho(\mathbf{R})e^{i\mathbf{q}\cdot\mathbf{R}}d\tau_R\right|^2, \quad (2)$$

where $\rho(\mathbf{R})$ is the nuclear charge distribution, normalized to unit volume integral.

In the case of inelastic scattering with small energy loss, Eq. (1) must be summed over all final states f that have excitation energies less than about 1 Mev.[2]

* Supported in part by the Office of Scientific Research, Air Research and Development Command.

† Sections 1, 2, and 7 revised in proof.

[1] Hofstadter, Fechter, and McIntyre, preceding paper [Phys. Rev. **92**, 978 (1953)]. See also Phys. Rev. **91**, 422 (1953).

[2] E. Guth, Anz. Akad. Wiss. Wien. Math.-naturw. Kl. **24**, 299–307 (1934); M. E. Rose, Phys. Rev. **73**, 279 (1948); J. H. Smith, Ph.D. Thesis, Cornell University, February, 1951 (unpublished); Thie, Mullin, and Guth, Phys. Rev. **87**, 962 (1952). Magnetic interactions may be ignored for the low nucleon energies involved here.

[3a] Yennie, Ravenhall, and Wilson, private communication. Earlier calculations by G. Parzen, Phys. Rev. **80**, 355 (1950) have been found to contain an error (private communications from E. Baranger and G. Parzen).

If we use the independent-particle model to estimate the ratio of inelastic to elastic scattering cross sections, only one term in the summation of Eq. (1) can enter for a particular final state (this assumes unsymmetrized nuclear wave functions, but the result is not greatly different if they are symmetrized). Also, such a matrix element will be somewhat smaller in the inelastic than in the elastic case, due to the partial interference between initial and final proton wave functions. Finally, not all of the protons in the nucleus can be excited if the final state must lie within 1 Mev of the ground state. If one considers all of these factors, one arrives at an estimate of between 0.01 and 0.1 for the ratio of inelastic to elastic scattering at a particular angle, in a heavy nucleus. On the other hand, recent experimental[3b] and theoretical[3c] work shows that quadrupole transition probabilities are ten to a hundred times larger than estimated above on the basis of the independent-particle model, for low-lying excited (collective rotational) states of heavy nuclei. This makes the inelastic cross section for favorable excited states comparable with the elastic cross section, and tends to smooth out oscillations in the computed form factor (see Sec. 3). Doubly magic Pb^{208}, which constitutes more than half of normal lead, is exceptional in that its first excited state lies more than 2.5 Mev above its ground state. Such an energy loss can be resolved by the experiments, so that it is unlikely that inelastic processes can account for the observed smoothness of the lead-scattering curve.

It is very difficult to estimate the effect of radiation on the observed scattering. The existing theory[4] is only useful for light elements and breaks down completely for large angle scattering from an element as heavy as gold. It does, however, indicate that the radiative correction does not depend strongly on energy loss and scattering angle. Experiments to date[1] show that most scattering events are only slightly inelastic, and it seems likely that this represents radiation loss rather than nuclear excitation.

The effect of the nuclear quadrupole is discussed more quantitatively in Sec. 6.

3. ELASTIC SCATTERING FROM HEAVY ELEMENTS USING BORN APPROXIMATION

We define the nuclear charge form factor as the integral which appears in the right side of Eq. (2):

$$F(\mathbf{q})=\int \rho(\mathbf{R})e^{i\mathbf{q}\cdot\mathbf{R}}d\tau_R. \qquad (3)$$

If $\rho(\mathbf{R})$ is real and spherically symmetric, $F(\mathbf{q})$ is also real and spherically symmetric. In this case, Eq. (3) can be written

$$F(q)=(4\pi/q)\int_0^\infty \rho(R)\sin(qR)RdR, \qquad (4)$$

and conversely

$$\rho(R)=(2\pi^2R)^{-1}\int_0^\infty F(q)\sin(qR)qdq. \qquad (5)$$

According to Eq. (2), $F(q)$ can be determined from the experimental observations:

$$F(q)=\pm[4E^2\sin^4\tfrac{1}{2}\theta\sigma(\theta)/Z^2e^4\cos^2\tfrac{1}{2}\theta]^{\frac{1}{2}},\quad q=(2E/\hbar c)\sin\tfrac{1}{2}\theta; \qquad (6)$$

here only the sign is indeterminate, and it can be inferred from the sign of $\rho(R)$ and the behavior of $F(q)$ near its zeros, if any. Thus, if accurate experiments were available over the entire range of q (0 to ∞), $\rho(R)$ could be determined uniquely from Eqs. (5) and (6), within of course the limits of the first Born approximation.

In practice, somewhat inaccurate experiments are available over a finite range of q. Also, no absolute values of $\sigma(\theta)$ have been measured as yet. The procedure followed in this paper consists in assuming a variety of forms for the charge density $\rho(R)$ and the corresponding form factor $F(q)$, and plotting the experimental values of $G(q)\equiv(\sin^2\tfrac{1}{2}\theta/\cos\tfrac{1}{2}\theta)\sigma^{\frac{1}{2}}(\theta)$ against q in such a way that an easily recognizable curve will result if $F(q)$ has the assumed form. This procedure makes consistent use of the first Born approximation. An alternative method, used by Hofstadter, Fechter, and McIntyre,[1] consists in defining the experimental form factor $G(q)$ as the square root of the ratio of the observed scattering to the exactly computed point-charge scattering rather than to the first Born approximation point-charge scattering. The optimum procedure probably lies somewhere between these two, since the first Born approximation is somewhat better for a finite nucleus than for a point nucleus, where the electrostatic potential is stronger. It is gratifying that the numerical results obtained here and in reference 1 are in such good agreement.

Suppose, for example, that it is desired to see how well the observations can be fitted with the assumption that the charge density is uniform over a sphere of radius R_0. In this case,

$$\rho(R)=\rho_0,\ R<R_0;\quad \rho(R)=0,\ R>R_0;$$
$$F(q)=4\pi\rho_0R_0^3[(\sin qR_0-qR_0\cos qR_0)/(qR_0)^3]. \qquad (7)$$

If then $F(q)$ is plotted against q on one sheet of log-log graph paper, and $G(q)$ is plotted against q on another sheet of log-log paper, superposition of the two will at once show the measure of agreement between Eq. (7) and the experimental observations. Vertical translation of the two sheets with respect to each other changes the absolute magnitude of the scattering, and horizontal translation changes the nuclear radius R_0.

[3b] T. Huus and Č. Zupančič, Kgl. Danske Videnskab. Selsk., Mat.-fys. Medd. **28**, 1 (1953); C. L. McClelland and C. Goodman, Phys. Rev. **91**, 760 (1953).
[3c] A. Bohr and B. Mottelson, Kgl. Danske Videnskab. Selsk., Mat.-fys. Medd. **27**, 16 (1953).
[4] J. Schwinger, Phys. Rev. **75**, 898 (1949).

A trial shows that the observations on gold do not fit unless it is assumed that the first minimum in the cross section expected theoretically is filled in by experimental inaccuracy, inelastic processes (Sec. 2), quadrupole moment effect (Sec. 6), or by higher order corrections to the Born approximation (Sec. 1). Even assuming that such a fill-in occurs, the rest of the experimental curve can only be fitted with a radius of about 4.7×10^{-13} cm, which is substantially smaller than that given by the usual expression $1.4\times10^{-13}A^{\frac{1}{3}}$ cm. Similar poor fits are obtained with the other elements.

The same technique was used to attempt a fit of the experiments with charge distributions that are uniform over most of the radius of the nucleus and rounded at the edge. If the usual radius is assumed, these predict diffraction minima and maxima that are not observed, as in the case of the sharp-edged uniform distribution. On the other hand, if the radius is assumed small enough to push the first diffraction minimum out to larger angles than are covered by the observations, the theoretically predicted small angle portion of the curve is too flat to agree with experiment. With sufficient rounding, the latter difficulty disappears; for example, the observations on gold can be fitted well with a charge distribution proportional to $[1+(R/a)^4]^{-1}$, where $a=3.3\times10^{-13}$ cm, but not with a charge distribution proportional to $[1+(R/a)^6]^{-1}$.

With charge distributions for which $F(q)$ has a simpler analytic form, a comparison with experiment can sometimes be achieved by plotting suitable functions of G and q against each other so that a straight line results when the experiments agree with the assumed form for $F(q)$. Four such forms are as follows:

$$\rho(R)=\rho_0\exp[-(R/a)^2]; \quad F(q)=\pi^{\frac{3}{2}}\rho_0 a^3\exp[-(qa/2)^2]. \quad (8)$$

$$\rho(R)=\rho_0 e^{-R/a}; \quad F(q)=8\pi\rho_0 a^3/(1+q^2a^2)^2. \quad (9)$$

$$\rho(R)=\rho_0[1+(R/a)]e^{-R/a}; \quad F(q)=32\pi\rho_0 a^3/(1+q^2a^2)^3. \quad (10)$$

$$\rho(R)=\rho_0 a^4/(a^2+R^2)^2; \quad F(q)=\pi^2\rho_0 a^3 e^{-qa}. \quad (11)$$

To fit Eq. (8), we plot G against q^2 on semilog graph paper; to fit Eq. (9), we plot $G^{-\frac{1}{2}}$ against q^2 on ordinary paper; to fit Eq. (10), we plot $G^{-\frac{1}{3}}$ against q^2 on ordinary paper; and to fit Eq. (11), we plot G against q on semilog paper. In each case, a straight line results if the fit is perfect, and the corresponding value of a is easily obtained.

A preliminary plot of G against q or q^2 on semilog paper shows that the experimental data for tantalum at 150 Mev and for gold and lead at 125 Mev can be superposed within the experimental errors for the separate elements by vertical translation (adjustment of the absolute magnitude of the scattering at some angle, which has not been measured). This is not surprising, since the values of $A^{\frac{1}{3}}$ for these three elements spread over a range of less than 5 percent. When all three elements are plotted together, it is found that a Gaussian charge distribution, Eq. (8), does not give a very good straight line. If a straight line is fitted to the whole curve, the value of a can lie between 3.1 and 3.6 (all lengths are expressed in units of 10^{-13} cm). The small-angle data are best fitted by $a=3.7$, and the large-angle data by $a=2.9$. If a Gaussian charge distribution is peaked enough (small enough a) at small R to fit the large-angle data, it falls off too rapidly at large R to give enough small-angle scattering; conversely, if it is spread out enough (large enough a) at large R to fit the small-angle data, it is too flat at small R to give enough large-angle scattering. The root-mean-square radius of the charge distribution for the Gaussian form is $R_s=(\frac{3}{2})^{\frac{1}{2}}a=1.224a$, so that R_s lies between 3.6 and 4.5 in this case.

The exponential charge distribution, Eq. (9), yields a fairly good straight line with $a=2.0$ (see Fig. 1), It is difficult to gauge the extreme values of a that are consistent with the experiments, because of the compression of the data that occurs in going from $\sigma(\theta)$ to $G^{-\frac{1}{2}}$. However, it is probably safe to say that a must lie between 1.6 and 2.9 on the basis of the present data. In this case, $R_s=(12)^{\frac{1}{2}}a=3.46a$, so that R_s lies between 5.5 and 10.0, with the best fit occurring at 6.9. The modified exponential charge distribution, Eq. (10), which has zero slope at the origin, also yields a straight line with $a=1.3$, and extreme values of 1.1 and 1.6. Here, $R_s=(18)^{\frac{1}{2}}a=4.24a$, so that R_s lies between 4.7 and 6.8, with the best fit occurring at 5.5. Finally, the

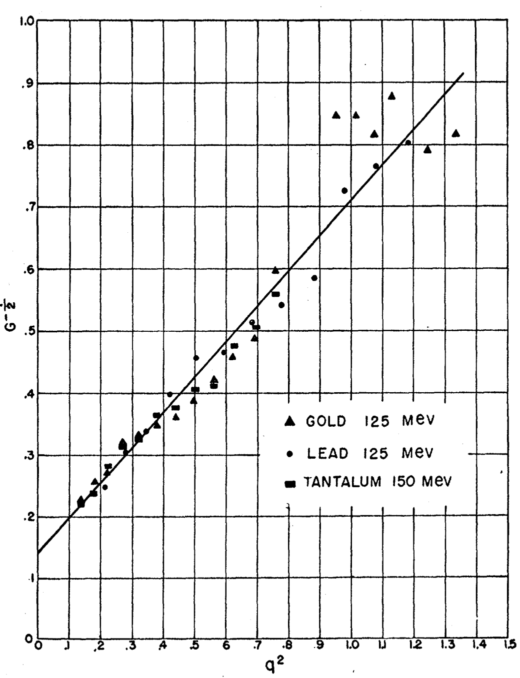

FIG. 1. Plot of $G^{-\frac{1}{2}}$ against q^2 (q in units of 10^{13} cm^{-1}), where G is the experimental form factor and $\hbar q$ is the momentum transfer. A straight line implies that the nuclear charge density has the form $\rho(R)=\rho_0 e^{-R/a}$. The line corresponds to $a=2.0\times10^{-13}$ cm.

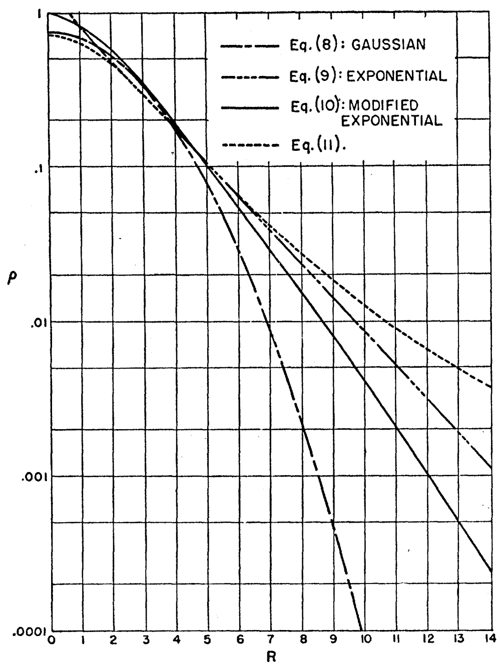

FIG. 2. Nuclear charge densities ρ computed from Eqs. (8), (9), (10), and (11) with optimum values of a. The last three are in good agreement between $R=2$ and $R=6$ (in units of 10^{-13} cm), but the first only agrees between $R=2$ and $R=4$.

charge distribution, Eq. (11), can be fitted well with $a=3.9\pm0.5$; because of its long tail, this distribution is rather unrealistic, and indeed R_s is infinite in this case.

The variety of shapes of charge distributions that fit the experiments about equally well suggests that only certain features of $\rho(R)$ are significant in this respect. This is confirmed when the above four charge densities are plotted against R on semilog graph paper, each with the optimum value of a. If the curves are translated vertically with respect to each other, it is found that Eqs. (9), (10), and (11) can be made to superpose within 15 percent over the region from $R=2$ to $R=6$ (see Fig. 2). The Gaussian distribution, Eq. (8), with $a=3.3$ can, however, only be fitted with the other three between $R=2$ and $R=4$. This suggests that the range of q covered in the experiments, from $q=0.37$ to $q=1.1$ (in units of 10^{13} cm^{-1}) is only sufficient to determine the shape of the nuclear charge distribution between $R=2$ and $R=6$. Very roughly and qualitatively, we can say that experiments with momentum transfers between $\hbar q_1$ and $\hbar q_2$ explore the shape of the charge distribution at distances between $R_2=2.2/q_2$ and $R_1=2.2/q_1$ from the center of the nucleus, provided that there is no anomalous behavior of $\rho(R)$ elsewhere.

4. ELASTIC SCATTERING FROM BERYLLIUM

The more limited experimental data on beryllium[1] at 125 Mev can be fitted well with any of the four charge distributions, Eqs. (8) through (11). The results are as follows:

$$\begin{aligned}
&\text{Eq. (8):} && a=1.8\ \pm0.1, && R_s=2.2\pm0.1;\\
&\text{Eq. (9):} && a=0.74\pm0.03, && R_s=2.7\pm0.1;\\
&\text{Eq. (10):} && a=0.55\pm0.01, && R_s=2.3\pm0.04;\\
&\text{Eq. (11):} && a=0.91\pm0.04, && R_s=\infty.
\end{aligned}$$

As with the heavier elements, Eqs. (10), (9), and (11) yield increasing values of a, and Eq. (9) gives a larger R_s than Eq. (10).

5. ELASTIC SCATTERING FROM DEUTERIUM

When Eq. (2) is applied to deuterium, it must be remembered that the ground state wave function is a mixture of $^3S_1$ and $^3D_1$ and is threefold degenerate. We write it[5]

$$\begin{aligned}\psi_m&=(4\pi)^{-\frac{1}{2}}r^{-1}(u+8^{-\frac{1}{2}}wS_{12})\chi_m,\quad m=0,\pm1,\\ S_{12}&=3r^{-2}(\boldsymbol{\sigma}_1\cdot\mathbf{r})(\boldsymbol{\sigma}_2\cdot\mathbf{r})-(\boldsymbol{\sigma}_1\cdot\boldsymbol{\sigma}_2),\end{aligned}\tag{12}$$

where χ_m is a triplet spin function. The normalization is such that

$$\int_0^\infty(u^2+w^2)dr=1.\tag{13}$$

Because of the degeneracy, the squared matrix element on the left side of Eq. (2) must be replaced by

$$\tfrac{1}{3}\sum_m\sum_{m'}\left|\int\psi_{m'}^*e^{\frac{1}{2}i\mathbf{q}\cdot\mathbf{r}}\psi_m d\tau\right|^2.\tag{14}$$

The factor $\frac{1}{2}$ in the exponent arises because the proton coordinate is half the relative coordinate that appears in Eq. (12). Equation (14) may be reduced to

$$\left[\int_0^\infty(u^2+w^2)j_0(\tfrac{1}{2}qr)dr\right]^2+\left[\int_0^\infty(2uw-2^{-\frac{1}{2}}w^2)j_2(\tfrac{1}{2}qr)dr\right]^2,\tag{15}$$

where

$$j_0(z)=z^{-1}\sin z,\quad j_2(z)=(3z^{-3}-z^{-1})\sin z-3z^{-2}\cos z$$

are spherical Bessel functions.

For use in connection with the next section, the expression for the quadrupole moment of the deuteron is quoted here[5]

$$Q=(200)^{-\frac{1}{2}}\int_0^\infty(2uw-2^{-\frac{1}{2}}w^2)r^2dr.\tag{16}$$

6. EFFECT OF NUCLEAR ELECTRIC QUADRUPOLE MOMENT

A nucleus that possesses an electric quadrupole moment is somewhat distorted from spherical shape, and we might expect that even if the charge distribution

[5] W. Rarita and J. Schwinger, Phys. Rev. 59, 436 (1941).

had a sharp edge, this edge would be effectively fuzzed out because the observations average the scattering produced by nuclei with all possible orientations.

In dealing with elastic scattering from a heavy nucleus, it is sufficient for a discussion of quadrupole moment effects to assume a charge distribution

$$\rho(\mathbf{R})=\rho_0(R)+\rho_2(R)P_2(\cos\theta), \tag{17}$$

where θ is the angle between the vector $\mathbf{R}$ and the nuclear axis, and $P_2(\mu)=\frac{1}{2}(3\mu^2-1)$ is a Legendre polynomial. The electric quadrupole moment measured with respect to an axis fixed in space that makes an angle θ' with the nuclear axis is

$$Q(\theta')=Z(8\pi/5)P_2(\cos\theta')\int_0^\infty \rho_2(R)R^4dR. \tag{18}$$

Equation (18) is classical, and from it we want to obtain an expression for the quadrupole moment Q, which can be related to the quantum analog of Eq. (18)[6]

$$Q(m)=\frac{3m^2-I(I+1)}{I(2I-1)}Q, \tag{19}$$

where I is the total angular momentum of the nucleus, and m is its component along the axis fixed in space. We could simply equate the maximum value $Q(0)$ of Eq. (18) to the maximum value $Q(I)$ of Eq. (19). However, a better comparison in the case of the deuteron (see below) is obtained if we equate the mean square computed from Eq. (18) by integrating over θ', to the mean square computed from Eq. (19) by summing over m. The result is

$$Q=A_IZ(8\pi/5)\int_0^\infty P_2(R)R^4dR, \tag{20}$$

where $A_1=(1/10)^{\frac{1}{2}}$, $A_{3/2}=(1/5)^{\frac{1}{2}}$, $A_2=(2/7)^{\frac{1}{2}}$, $A_{5/2}=(5/14)^{\frac{1}{2}}$, $A_3=(5/12)^{\frac{1}{2}}$, $A_{7/2}=(7/15)^{\frac{1}{2}}$, $\cdots A_\infty=1$.

In calculating the scattering, we make use of the fact that the period of rotation of the nucleus is large in comparison with the transit time of a fast electron across the nucleus. Thus, the form factor calculated from Eq. (3) refers to a particular orientation of the nucleus with respect to $\mathbf{q}$. The scattering, which is proportional to F^2, must then be averaged over all orientations of the nucleus. It is easily shown that

$$\langle F^2(q)\rangle_{\text{Av}}=16\pi^2\left[\int_0^\infty \rho_0(R)j_0(qR)R^2dR\right]^2 +(16\pi^2/5)\left[\int_0^\infty \rho_2(R)j_2(qR)R^2dR\right]^2, \tag{21}$$

which agrees with Eq. (4) if $\rho_2=0$.

[6] J. M. Blatt and V. F. Weisskopf, *Theoretical Nuclear Physics* (John Wiley and Sons, Inc., New York, 1952), p. 28.

It is interesting to compare Eqs. (17), (20), and (21) with the corresponding Eqs. (13), (16), and (15) for the deuteron (Sec. 5), when it is remembered that $\rho(R)$ is normalized to unit volume integral. We note that $\mathbf{R}=\frac{1}{2}\mathbf{r}$; then if $4\pi\rho_0R^2dR$ is identified with $(u^2+w^2)dr$, and $(16\pi^2/5)^{\frac{1}{2}}\rho_2R^2dR$ is identified with $(2uw-2^{-\frac{1}{2}}w^2)dr$, the normalization of $\rho(\mathbf{R})$ in Eq. (17) agrees with Eq. (13), (21) agrees with (15), and (20) agrees with (16).

We can now see under what circumstances the second term on the right side of Eq. (21) can fill in the first diffraction minimum of the first term, that is predicted by a sharp-edged uniform charge distribution. We assume that $\rho_0(R)=\rho_0$, a constant, out to $R=R_0$, and is zero for larger values of R. We also assume, as is justified if the quadrupole moment or the eccentricity is not too large, that $\rho_2(R)=B\delta(R-R_0)$. Then B can be expressed in terms of Q from Eq. (20):

$$Q=A_IZ(8\pi/5)BR_0^4.$$

It is convenient to define the nuclear eccentricity[7] $\eta\equiv5Q/4R_0^2Z$, in which case Eq. (21) can be written

$$\langle F^2(q)\rangle_{\text{Av}}=9(\sin qR_0-qR_0\cos qR_0)^2/(qR_0)^6 +4\eta^2j_2^2(qR_0)/5A_I^2, \tag{22}$$

when it is remembered that $4\pi\rho_0R_0^3/3=1$.

The first term on the right side of Eq. (22) vanishes when $qR_0\cong4.5$, and has its second maximum at $qR_0\cong6$, where it is equal to 7.0×10^{-3}. At the zero point of the first term, the second term is equal to $0.038(\eta/A_I)^2$. We can say that the zero predicted when the quadrupole moment is neglected would be difficult to observe as a minimum if the second term had there a value comparable with the value of the first term at its second maximum, that is, if $0.038(\eta/A_I)^2\cong7.0\times10^{-3}$, or if $(\eta/A_I)\cong0.43$. For Ta^{181}, $\eta=0.14$ (one of the largest values known) and $I=7/2$, so that $(\eta/A_I)=0.205$. For Au^{197}, $I=3/2$, and the quadrupole moment has not been measured; however, it would have to be extremely large to be effective in the present connection, and this seems unlikely from other considerations. Three-quarters of normal lead consists of the isotopes Pb^{208} $(I=0)$ and Pb^{207} $(I=\frac{1}{2})$, neither of which can have a quadrupole moment. It seems probable, therefore, that a nuclear electric quadrupole moment cannot account for the smoothness of the observed scattering curves.

7. CONCLUDING REMARKS

The picture of the nuclear charge distribution arrived at on the basis of the Born approximation is radically different from that which has been commonly accepted until now.[8] However, such centrally peaked, smoothly tapering charge distributions are not necessarily inconsistent with information obtained from other types of

[7] Reference 6, p. 26.

[8] A slight indication of a central charge concentration was obtained from the scattering of 15.7-Mev electrons, by Lyman, Hanson, and Scott [Phys. Rev. 84, 626 (1951)].

experiments. As an example, any experiment that measures the average value of the difference between the actual electrostatic potential and that of an equal point charge, measures in effect the root-mean-square radius R_s of the charge distribution. For a uniform charge distribution of radius R_0, $R_s=(3/5)^{\frac{1}{2}}R_0=0.775R_0$. This gives R_s values ranging from 6.14 for tantalum to 6.42 for lead, if the usual expression $R_0=1.4A^{\frac{1}{3}}$ is used; for beryllium, $R_s=2.25$. It is apparent from Sec. 3 that the heavy elements are consistent with this if either Eq. (9) or Eq. (10) is used. In the case of beryllium (Sec. 4), the values found from Eqs. (8) and (10) are consistent with that obtained from the $A^{\frac{1}{3}}$ rule, and Eq. (9) yields a somewhat larger value; for such a light nucleus, the $A^{\frac{1}{3}}$ rule probably underestimates the radius.

The nuclear Coulomb energy may be calculated for each of the charge distributions considered here. It is characterized by a length, which is equal to the ratio of the square of the total charge to the Coulomb energy. This length is $(5/3)R_0$ for a uniform charge distribution of radius R_0, $(2\pi)^{\frac{1}{2}}a$ for the Gaussian distribution (8), $(32/5)a$ for the exponential distribution (9), $(512/63)a$ for the distribution (10), and $(\pi/2)a$ for the distribution (11). With the optimum values for a, the distributions (9) and (10) are 5 and 14 percent, respectively, higher than the Coulomb energy calculated with $R_0=1.4A^{\frac{1}{3}}$, while the other two distributions give about twice as large a Coulomb energy. Thus, as with the root-mean-square radius, the more likely charge distributions (9) and (10) are in satisfactory agreement with earlier results.

It is important also to realize that electron scattering and nucleon scattering measure quite different properties of a nucleus. We have assumed here that electron scattering is determined by the electric charge density, which is equivalent to assuming that there is no appreciable non-electric interaction of electrons and nuclear matter. Since lower energy scattering experiments are in good agreement with this assumption,[9] any anomalous interaction would have to be strongly momentum-dependent in order to be significant in the present situation, and we suppose that such an interaction does not exist. According to present ideas, the electric charge density is proportional to the density of protons, since meson charges are expected to average to zero. Nucleon scattering, on the other hand, is determined by the nucleonic potential, which is believed to depend on the nucleon density but need not be proportional to it. Indeed, it is quite possible that this potential is proportional to the density only for quite low densities, and that for higher densities the potential increases less rapidly than linearly.[10] In this case, the potential that is effective in nucleon scattering will be more nearly uniform and have a sharper boundary than the electric charge density, and hence make the nucleus appear more like a uniform sphere. This might explain the agreement between the usual R_0 and the nuclear radius measured from fast neutron scattering and alpha-particle decay, and also the very striking diffraction patterns recently observed in the scattering of 22-Mev protons by various elements.[11]

It is, of course, possible that exact calculations will fit the experimental observations on electron scattering with charge distributions that are less peaked at the center and fall off more sharply at the edge of the nucleus. Such calculations are now under way here, and will be reported in the near future by D. R. Yennie, D. G. Ravenhall, and R. N. Wilson.

It is a pleasure to acknowledge numerous discussions with Professor R. Hofstadter on the experimental information and his treatment of it. The writer is also indebted to Professors R. F. Christy, E. Guth, W. E. Lamb, E. Teller, and C. H. Townes for helpful conversations, and to Mr. K. G. Dedrick for aid with one aspect of the calculations.

[9] See reference 8, and Buechner, Van de Graaff, Sperduto, Burrill, and Feshbach, Phys. Rev. **72**, 678 (1947).

[10] L. I. Schiff, Phys. Rev. **84**, 1 (1951); B. J. Malenka, Phys. Rev. **86**, 68 (1952); W. E. Thirring, Z. Naturforsch. **7a**, 63, 279 (1952).

[11] B. L. Cohen and R. V. Neidigh, Phys. Rev. (to be published). The author is indebted to Dr. A. M. Weinberg for informing him of these results prior to publication.